Simulation of copper–water nanofluid in a microchannel in slip flow regime using the lattice Boltzmann method with heat flux boundary condition

2015 J. Phys.: Conf. Ser. 655 012029

(http://iopscience.iop.org/1742-6596/655/1/012029)

Journal of Physics: Conference Series **655** (2015) 012029 doi:10.1088/1742-6596/655/1/012029

Simulation of copper–water nanofluid in a microchannel in slip flow regime using the lattice Boltzmann method with heat flux boundary condition

A D'Orazio[1], Z Nikkhah[2], A Karimipour[2]

[1] Dipartimento di IngegneriaAstronautica, Elettrica ed Energetica, Sapienza Università di Roma, Via Eudossiana 18, Roma 00184, Italy
[2] Department of Mechanical Engineering, Najafabad Branch, Islamic Azad University, Isfahan, Iran, Postal Code: 8196848531

E-mail:annunziata.dorazio@uniroma1.it

Abstract. Laminar forced convection heat transfer of water–Cu nanofluids in a microchannel is studied using the double population Thermal Lattice Boltzmann method (TLBM). The entering flow is at a lower temperature compared to the microchannel walls. The middle section of the microchannel is heated with a constant and uniform heat flux, simulated by means of the counter slip thermal energy boundary condition. Simulations are performed for nanoparticle volume fractions equal to 0.00%, 0.02% and 0.04% and slip coefficient equal to 0.001, 0.01 and 0.1. Reynolds number is equal to 1, 10 and 50.The model predictions are found to be in good agreement with earlier studies. Streamlines, isotherms, longitudinal variations of Nusselt number and slip velocity as well as velocity and temperature profiles for different cross sections are presented. The results indicate that LBM can be used to simulate forced convection for the nanofluid micro flows. They show that the microchannel performs better heat transfers at higher values of the Reynolds number. For all values of the Reynolds considered in this study, the average Nusselt number increases slightly as the solid volume fraction increases and the slip coefficient increases. The rate of this increase is more significant at higher values of the Reynolds number.

1. Introduction

The lattice Boltzmann Equation (LBE) is a minimal form of the Boltzmann kinetic equation, which is the evolution equation for a continuous one-body distribution function, wherein all details of molecular motion are removed except those that are strictly needed to represent the hydrodynamic behaviour at the macroscopic scale; it has gained much attention for its ability to simulate fluid flows, and for its potential advantages over conventional numerical solution of the Navier–Stokes equations.

[1] To whom any correspondence should be addressed

The kinetic nature of Lattice Boltzmann Method (LBM) introduces key advantages, including easy implementation of boundary conditions and fully parallel algorithms. In addition, the convection operator is linear, no Poisson equation for the pressure must be resolved and the translation of the microscopic distribution function into the macroscopic quantities consists of simple arithmetic calculations [1]. LBM have met with significant success for the numerical simulation of a large variety of fluid flows, including real-world engineering applications and physical phenomena of various complexities as multiphase flows, complex geometries and interfacial flows [2]. The application to fluid flow coupled with non negligible heat transfer turned out to be much more difficult. The LBE thermal models fall into three categories: the multi-speed approach, the passive scalar approach and the doubled populations approach. In this latter, successful, strategy thermal energy density and heat flux are expressed as kinetic moments of a thermal distribution function, so that no kinetic moment beyond the first order is ever required, thus providing numerical stability, also in case of significant temperature gradient [3]; in addition, with respect to the previous approaches, viscous heat dissipation and compression work done by the pressure were naturally incorporated and the boundary conditions are easily implemented because both populations live in the same lattice, where additional speeds are not necessary.

During the last two decades, much attention has been paid to make and use micro devices. The small sizes as well as high efficiency of micro devices – such as microsensors, microvalves and micropumps – are some of the advantages of using MEMS and NEMS (Micro and Nano Electro Mechanical Systems). To guarantee the performance of such devices and make them cool, many studies have been carried out concerning flow and heat transfer in microchannels. At micro scale level, the surface effects are getting more important which leads to change in the classic boundary conditions. The well known differences of micro flows from the macroscopic ones are the slip velocity and temperature jump on the solid–fluid boundaries. For the gas micro flows, the flow regimes can be slip, transient and free molecular flow regimes; however for liquid micro flows, mainly the slip flow regime can be observed [4]. Therefore, in addition to classic Navier–Stokes (NS), the particle-based methods including direct simulation of Monte Carlo (DSMC), molecular dynamics (MD) and the lattice Boltzmann method (LBM) may be applied [5]. Expensive computation cost and complex mathematical procedure of MD and DSMC, as well as the inability of N–S for simulation of flow in transition and free molecular regimes, have encouraged the researchers to use LBM.

On the other hand, using nanofluids is an innovative way to increase heat transfer which has attracted the researchers' interests who are working on micro flow due to their exciting potential. Nanofluids are a mixture of liquid and dispersed solid nanoparticles. The higher thermal conductivity of nanoparticles leads to the increase of nanofluid heat transfer. Nanofluid's characteristics are different from the traditional solid–liquid mixtures in milli or micro-meter particle's size. There are many studies concerning nanofluid in cavities and tubes which involve its positive effects on the Nusselt number. Some researchers have reported the flow and heat transfer of the nanofluid in microchannels [6-9]. For instance, Raisi et al. [10] simulated the Cu–water nanofluid in a microchannel for both slip and no-slip conditions, ignoring the temperature jump effects and applying the classic Navier–Stokes equations. All in all, theoretical results of fluid flow in slip flow regimes or even simulation of nanofluid flow using LBM (in single phase or multi-phase mixture model) have been presented by several researchers. However, there are few studies concerning nanofluid simulation in microchannels using LBM [11-13]. However, all of them have ignored the slip velocity and temperature jump effects. The open literature suggests that nanofluids are an effective coolant which requires more investigations. In particular, the convection heat transfer of nanofluids in microchannel in the slip flow regime is still not entirely understood.

In the present study, laminar forced convection heat transfer of dilute water–Cu nanofluids in a microchannel is analyzed. The double population Thermal Lattice Boltzmann method (TLBM) is used.

The middle section of the microchannel is heated with a constant and uniform heat flux. This type of boundary condition, representing very usual situations in physical world, is not simple to model in lattice Boltzmann schemes. In effect, the only boundary condition able to simulate imposed temperature and imposed heat flux at a boundary is the counter-slip thermal energy density boundary condition, that has been presented by D'Orazio et al. in [3, 19, 20] (where the boundary were at rest), and used in case of moving wall in [14]. The results obtained in this work are weighed against model validation results found in the literature. Particular attention is paid to the effects of different slip velocities (slip coefficient is equal to 0.001, 0,01 and 0.1) and different solid volume fractions (equal to 0.00%, 0,02% and 0.04%). Reynolds number is equal to 1, 10 and 50. The model predictions are found to be in good agreement with earlier studies.

2. Thermal and hydrodynamic Lattice Boltzmann Method

The lattice Boltzmann equation with a single relaxation time from the BGK model can be expressed as

$$\tilde{f}_i(\vec{x}+\vec{c}_i dt, t+dt) - \tilde{f}_i(\vec{x},t) = -\frac{dt}{\tau_f+0.5dt}\left[\tilde{f}_i - \tilde{f}_i^e\right] \tag{1}$$

$$\tilde{g}_i(\vec{x}+\vec{c}_i dt, t+dt) - \tilde{g}_i(\vec{x},t) = -\frac{dt}{\tau_g+0.5dt}\left[\tilde{g}_i - \tilde{g}_i^e\right] - \frac{\tau_g dt}{\tau_g+0.5dt} f_i Z_i \tag{2}$$

where the populations $\tilde{f}_i$ carry mass and momentum and the populations $\tilde{g}_i$ carry internal energy and heat flux. The discrete distribution functions $\tilde{f}_i$ and $\tilde{g}_i$ are introduced as in [5]:

$$\tilde{f}_i = f_i + \frac{dt}{2\tau_f}(f_i - f_i^e) \tag{3}$$

$$\tilde{g}_i = g_i + \frac{dt}{2\tau_g}(g_i - g_i^e) + \frac{dt}{2} f_i Z_i \tag{4}$$

$$Z_i = (\vec{c}_i - \vec{u}) D_i \vec{u}\ , \quad D_i = \partial_t + \vec{c}_i \cdot \nabla \tag{5}$$

where f_i and g_i are the discrete populations which evolve when a standard first order integration strategy is adopted, the terms Z_i and D_i represent the effects of viscous heating and the material derivative along direction $\vec{c}_i$ respectively, τ_f and τ_g are relaxations times and f_i^e and g_i^e are the equilibrium distribution functions. Throughout of this work, two-dimensional square lattice with the nine speeds, as shown in figure 1, is used.

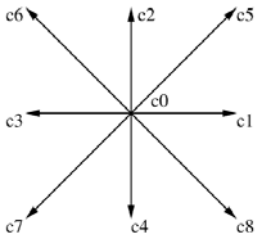

Figure 1. Nine-speed square lattice.

The discrete particle lattice speeds are:

$$c_i = \left(cos\frac{i-1}{2}\pi, sin\frac{i-1}{2}\pi\right)c, \qquad i = 1,2,3,4 \tag{6}$$

$$c_0 = (0,0) \qquad c_i = \sqrt{2}\left[cos\left(\frac{i-5}{2}\pi + \frac{\pi}{4}\right), sin\left(\frac{i-5}{2}\pi + \frac{\pi}{4}\right)\right]c, \qquad i = 5,6,7,8 \tag{7}$$

where $c^2 = 3RT$ and T is the temperature. The equilibrium density distributions are chosen as follows:

$$f_i^e = \omega_i \rho \left[1 + \frac{3\vec{c}_i \cdot \vec{u}}{c^2} + \frac{9(\vec{c}_i \cdot \vec{u})^2}{2c^4} - \frac{3(u^2+v^2)}{2c^2}\right] \quad (8)$$

$$g_0^e = -\omega_0 \left[\frac{3\rho e(u^2+v^2)}{2c^2}\right] \quad (9)$$

$$g_{1,2,3,4}^e = \omega_1 \rho e \left[1.5 + 1.5\frac{\vec{c}_i \cdot \vec{u}}{c^2} + 4.5\frac{(\vec{c}_i \cdot \vec{u})^2}{c^4} - 1.5\frac{(u^2+v^2)}{c^2}\right] \quad (10)$$

$$g_{5,6,7,8}^e = \omega_2 \rho e \left[3 + 6\frac{\vec{c}_i \cdot \vec{u}}{c^2} + 4.5\frac{(\vec{c}_i \cdot \vec{u})^2}{c^4} - 1.5\frac{(u^2+v^2)}{c^2}\right] \quad (11)$$

where $\vec{u} = (u, v)$ and $\rho e = \rho RT$ (in two-dimensional geometry). The weights of the different populations are

$$\omega_0 = \frac{4}{9} \qquad \omega_i = \frac{1}{9} \;\; i = 1,2,3,4 \qquad \omega_i = \frac{1}{36} \quad i = 5,6,7,8 \quad (12)$$

The terms enclosed by the square bracket, multiplied by the corresponding weights ω_i, will be called *corresponding form for equilibrium*.

Finally, using f_i^e and g_i^e, hydrodynamic and thermal variables are calculated as follows:

$$\rho = \sum_i \tilde{f}_i \qquad \rho e = \sum_i \tilde{g}_i - \frac{dt}{2}\sum_i f_i Z_i \quad (13)$$

$$\rho\vec{u} = \sum_i \vec{c}_i \tilde{f}_i \qquad \vec{q} = \left[\sum_i \vec{c}_i \tilde{g}_i - \rho e\vec{u} - \frac{dt}{2}\sum_i \vec{c}_i f_i Z_i\right]\frac{\tau_g}{\tau_g + 0.5dt} \quad (14)$$

The kinematic viscosity and the thermal diffusivity in the two-dimensional geometry are given by:

$$\nu = \tau_f R\bar{T}, \qquad \chi = 2\tau_g R\bar{T} \quad (15)$$

3. Nanofluid

Nanofluid is a homogeneous mixture of the liquid and suspended nanoparticles. Its effective density can be obtained by

$$\rho_{nf} = \varphi\rho_s + (1-\varphi)\rho_f \quad (16)$$

where φ is the nanoparticle volume fraction and the subscripts "f", "s" and "nf" refer to base fluid, solid nanoparticles and nanofluid, respectively. Using the heat capacity of nanofluid, the nanofluid thermal diffusivity can be obtained by [15]:

$$(\rho C_p)_{nf} = \varphi(\rho C_p)_s + (1-\varphi)(\rho C_p)_f \qquad \alpha_{nf} = k_{nf}/(\rho C_p)_{nf} \quad (17)$$

The effective dynamic viscosity is expressed by using the Brinkman model [16]:

$$\mu_{nf} = \mu_f/(1-\varphi)^{2.5} \quad (18)$$

Following equation, which was presented by Patel et al. [17,18], is considered to determine the nanofluid thermal conductivity k_{nf} as a function of liquid and solid thermal conductivities

$$k_{nf}/k_f = 1 + \left[\frac{k_s}{k_f}\frac{A_s}{A_f} + Ck_s Pe\frac{A_s}{k_f A_f}\right] \quad (19)$$

in which

$$\frac{A_s}{A_f} = \frac{d_f}{d_s}\frac{\varphi}{1-\varphi} \qquad Pe = \frac{u_B d_s}{\alpha_f} \qquad u_B = \frac{2k_B T}{\pi\mu_f d_s^2} \qquad k_B = 1.3807\times10^{-23}\,J/K \qquad C = 36000 \quad (20)$$

where Pe is the Péclet number with the Brownian motion velocity of particles u_B and k_B is the constant of Boltzmann.

4. Boundary conditions

Non-equilibrium bounce back model, normal to the boundary, is used for inlet and outlet hydrodynamic boundary conditions. In this model, distribution functions are reflected in suitable ways to satisfy the equilibrium conditions and improve accuracy. It results

$$\tilde{f}_1 = \tilde{f}_3 + \frac{2}{3}\rho_i U_i \qquad \tilde{f}_5 = \tilde{f}_7 + \frac{1}{2}\left(\tilde{f}_4 - \tilde{f}_2\right) + \frac{1}{6}\rho_i U_i \qquad \tilde{f}_8 = \tilde{f}_6 - \frac{1}{2}\left(\tilde{f}_4 - \tilde{f}_2\right) + \frac{1}{6}\rho_i U_i \tag{21}$$

$$\tilde{f}_3 = \tilde{f}_1 - \frac{2}{3}\rho_{out} U_{out} \tag{22}$$

$$\tilde{f}_7 = \tilde{f}_5 - \frac{(\tilde{f}_4 - \tilde{f}_2)}{2} - \frac{\rho_{out} U_{out}}{6} - \frac{\rho_{out} V_{out}}{2} \qquad \tilde{f}_6 = \tilde{f}_8 + \frac{(\tilde{f}_4 - \tilde{f}_2)}{2} - \frac{\rho_{out} U_{out}}{6} + \frac{\rho_{out} V_{out}}{2} \tag{23}$$

With regard to thermal boundary conditions at inlet and outlet sections, they are obtained by means a thermal counter-slip approach as proposed by [3,19,20], in which the incoming unknown thermal populations are assumed to be equilibrium distribution functions with a counter slip thermal energy density e', which is determined so that suitable constraints are verified. It results

$$\tilde{g}_1 = \frac{6\rho e + 3dt\sum_i f_i Z_i - 6(\tilde{g}_0 + \tilde{g}_2 + \tilde{g}_3 + \tilde{g}_4 + \tilde{g}_6 + \tilde{g}_7)}{2 + 3U_i + 3U_i^2} \times \left[1.5 + 1.5U_i + 3U_i^2\right]\frac{1}{9} \tag{24}$$

$$\tilde{g}_5 = \frac{6\rho e + 3dt\sum_i f_i Z_i - 6(\tilde{g}_0 + \tilde{g}_2 + \tilde{g}_3 + \tilde{g}_4 + \tilde{g}_6 + \tilde{g}_7)}{2 + 3U_i + 3U_i^2} \times \left[3 + 6U_i + 3U_i^2\right]\frac{1}{36} \tag{25}$$

$$\tilde{g}_8 = \frac{6\rho e + 3dt\sum_i f_i Z_i - 6(\tilde{g}_0 + \tilde{g}_2 + \tilde{g}_3 + \tilde{g}_4 + \tilde{g}_6 + \tilde{g}_7)}{2 + 3U_i + 3U_i^2} \times \left[3 + 6U_i + 3U_i^2\right]\frac{1}{36} \tag{26}$$

$$\tilde{g}_3 = \frac{6(\tilde{g}_1 + \tilde{g}_5 + \tilde{g}_8) - 3dt\sum_i c_{ix} f_i Z_i - 6\rho e u_{out}}{2 - 3U_{out} + 3U_{out}^2} \times \left[1.5 - 1.5U_{out} + 3U_{out}^2 - 1.5V_{out}^2\right]\frac{1}{9} \tag{27}$$

$$\tilde{g}_6 = \frac{6(\tilde{g}_1 + \tilde{g}_5 + \tilde{g}_8) - 3dt\sum_i c_{ix} f_i Z_i - 6\rho e U_{out}}{2 - 3U_{out} + 3U_{out}^2} \times \left[3 - 6U_{out} + 6V_{out} + 3U_{out}^2 + 3V_{out}^2 - 9U_{out}V_{out}\right]\frac{1}{36} \tag{28}$$

$$\tilde{g}_7 = \frac{6(\tilde{g}_1 + \tilde{g}_5 + \tilde{g}_8) - 3dt\sum_i c_{ix} f_i Z_i - 6\rho e U_{out}}{2 - 3U_{out} + 3U_{out}^2} \times \left[3 - 6U_{out} - 6V_{out} + 3U_{out}^2 + 3V_{out}^2 + 9U_{out}V_{out}\right]\frac{1}{36} \tag{29}$$

With regard to microchannel walls boundary conditions, the slip boundary condition is applied for hydrodynamic field. More specifically, we refer to the work of Ngoma and Erchiqui [21] who considered the slip length coefficient β and defined the slip velocity u_s for the liquid inside the microchannel on the stationary walls and we write the dimensionless slip velocity U_s as

$$u_s = \pm\beta \left.\frac{\partial u}{\partial y}\right|_{y=0,h} \qquad U_s = \pm B \left.\frac{\partial U}{\partial Y}\right|_{Y=0,1} \tag{30}$$

To determine the slip velocity in LBM, the specular reflective bounce back model (combination of bounce back and specular boundary condition) is applied in this work. For example for the bottom wall, the unknown distribution functions are estimated by

$$\tilde{f}_2 = \tilde{f}_4 \qquad \tilde{f}_5 = r\tilde{f}_7 + (1-r)\,\tilde{f}_8 \qquad \tilde{f}_6 = r\tilde{f}_8 + (1-r)\,\tilde{f}_7 \tag{31}$$

The accommodation coefficient value, r, is chosen appropriately for more accuracy [22].
With regard to thermal boundary conditions at the microchannel walls, the middle section of the microchannel is heated with a constant and uniform heat flux, whereas the final section is insulated. These boundary conditions are obtained by means of the thermal counter-slip approach with imposed

heat flux. As an example, for the top wall of the channel, named as "north wall", in which entering heat flux is constant and equal to q_N, the unknown $\tilde{g}_4$, $\tilde{g}_7$ and $\tilde{g}_8$ are chosen as follows.

$$\tilde{g}_i = \rho(e_N + e') \times [corresponding\ form\ for\ equilibrium] \qquad i = 4,7,8 \tag{32}$$

By definition:

$$\sum_i c_{iy}\, \tilde{g}_i = \frac{dt}{2}\sum_i c_{iy} f_i Z_i + \rho e_N V_N + \frac{\tau_g + 0.5dt}{\tau_g} q_y \tag{33}$$

which yields to:

$$\rho e_N + \rho e' = \left[K - \frac{dt}{2}\sum_i \frac{c_{iy}}{c} f_i Z_i - \rho e_N \frac{V_N}{c} - \frac{\tau_g + 0.5dt}{\tau_g}\frac{q_y}{c}\right] \Big/ \left[\frac{1}{3} - \frac{1}{2}\frac{V_N}{c} + \frac{1}{2}\frac{V_N^2}{c^2}\right] \tag{34}$$

where V_N is the component normal to the wall of flow velocity at the wall, K is the sum of the three known populations ($\tilde{g}_2$, $\tilde{g}_5$ and $\tilde{g}_6$) e_N denotes the current value of thermal energy density at the north wall. The numerical value of the heat flux q_N (and similarly for the value q_S at the south wall) is obviously equal to zero for the final section of the microchannel. The corners nodes are treated similarly and the counter-slip procedure can be applied to the five unknown incoming populations at the corner. The same relations are used for the bottom wall (named as "south wall"), in which entering heat flux is constant and equal to q_S and the unknown populations are $\tilde{g}_2$, $\tilde{g}_5$ and $\tilde{g}_6$.
With regard to the initial conditions, the velocities of all nodes inside the cavity are taken as zero initially. The initial density is set to a value of 2.7. The initial equilibrium distribution functions are evaluated correspondingly. The initial distribution functions are taken as the corresponding equilibrium values.

5. Results and discussion

Laminar forced convection heat transfer of a Cu–water nanofluid in a long microchannel is studied numerically using Lattice Boltzmann Method previously described. Length L and height H are shown in Figure 2. The top and bottom walls are partially heated; nanofluid enters the microchannel with inlet velocity and temperature u_i and T_i respectively.

The nanofluid simulated in this work is a dispersion of nanoparticles of copper (Cu) in pure water (as the base liquid). It is assumed that the considered fluid is a Newtonian, incompressible fluid, in laminar flow regime. Nanoparticles are spherical, with diameter as $d_p = 100\text{nm}$. Water and nanoparticles mixture is in the homogeneous mode and the radiation effect is negligible.

Characteristic dimensionless number in the analysis of laminar forced convection problems of nanofluids in microchannels are the Reynolds number and Prandtl numbers, defined as $\text{Re} = u_i h/\nu_f$ and $\text{Pr} = \nu_f/\alpha_f$ respectively, nanoparticle concentration φ and slip coefficient B. As stated before, lattice Boltzmann method is used for near-incompressible flows and therefore Mach number is assumed as $\text{Ma} \ll 1$. More specifically, the characteristic velocity of the flow must be small compared with the fluid speed of sound; in present study the velocity u_i is selected as $u_i = 0.1c$ ($U_i = 0.1$). The Prandtl number is calculated for the nanofluid mixture at $\varphi = 0$ (pure water), $\varphi = 0.02$ and $\varphi = 0.04$ and the and Reynolds number is assumed as $Re = 1$, $Re = 10$ and $Re = 50$. The effects of the slip velocity on the flow and heat transfer are studied; the slip velocity coefficient is assumed as $B = 0.001$, $B = 0.01$ and $B = 0.1$.

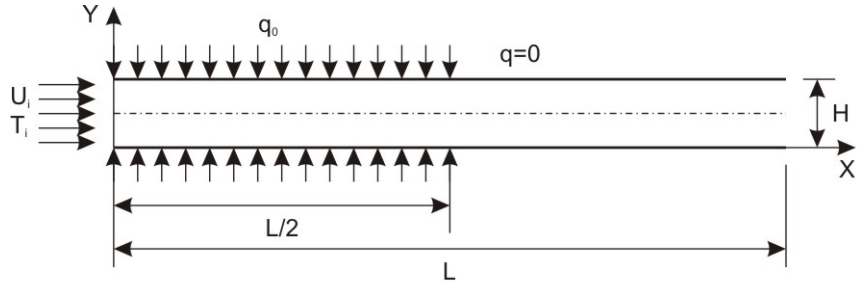

Figure 2. The schematic diagram of the microchannel.

To avoid ambiguity, the boundary of the channel are referred to according to the coordinates shown in Figure 2. In the following the macroscopic variables of fluid flow are made dimensionless as follows, respectively for dimensionless coordinates, velocity components, temperature, time

$$Y = \frac{y}{H}\,, \quad X = \frac{x}{H}\,, \quad L = \frac{l}{H}\,, \quad U = \frac{u}{U_i}\,, \quad V = \frac{v}{U_i}\,, \quad \Theta = \frac{T-T_i}{\Delta T}\,, \quad \Delta T = \frac{q_y H}{k_f}\,, \quad \tau = \frac{tU_i}{H} \tag{35}$$

Therefore, the local and average Nusselt numbers along the microchannel wall are calculated using following relations

$$Nu_X = \frac{\lambda H}{k_f} = \frac{q_y H}{k_f\,(T_s - T_i)} = \frac{\Delta T}{(T_s - T_i)} = \frac{1}{\Theta_s(X)}\,, \qquad Nu_m = \frac{1}{L}\int_0^L Nu_X dX \tag{36}$$

where $\lambda = q_y/(T_s - T_i)$ is the convection coefficient. The top wall is the at $Y = 1$, the bottom wall is at Y=0 and the inlet and outlet sections are at $X = 0$ and $X = 32$.

In order to obtain grid independent solution, a grid refinement study is performed for nanoparticle concentration $\varphi = 0.02$ and slip coefficient $B = 0.001$. Grid independence of the results is established in term of average Nusselt number on the wall and dimensionless maximum value of temperature Θ at and $Y = 0.1$ for three different grid size, namely 40×400, 50×500 and 60×600 lattice nodes; due to small difference between the results of the last two grid sizes, the 50×500 grid is chosen as a suitable one in this work.

To validate the computer code, the comparison with the values obtained by Raisi et al. [10] for the longitudinal velocity U_{out} at the end of the microchannel is examined for the slip coefficient equal to 0.05 and 0.1 and nanoparticles concentration coefficient and Reynolds number equal to 0.03 and 50.0 respectively; in addition, the comparison with the values obtained by Aminossadati et al. [7] for the average Nusselt number Nu_m is examined for the Reynolds number equal to 10.0, 100.0 and 500.0. The values obtained in present work show good agreement with those in [10] and [7], with a maximum error equal to 0.2% and 1.9% respectively.

In order to show the effect of the Reynolds number on the flow field and heat transfer, in Figures 3, 4 and 5 streamlines and isotherms are reported for slip velocity coefficient $B = 0.1$ and nanoparticles concentration coefficient $\varphi = 0.02$ for the cases $Re = 1$, 10 and 50. Nanofluid enters the microchannel from the left and after cooling the walls, it leaves from the right side. So, there will be symmetric and horizontal streamlines along the microchannel. For the same values of Reynolds number in Figure 6, 7 and 8 the slip velocity U_s is reported as a function of the slip coefficient. It can be observed that at the inlet, the slip velocities start from their maximum values and decrease asymptotically along the wall and approach constant values; larger B corresponds to larger slip velocity on the walls.

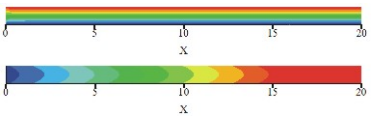

Figure 3. Streamlines (top) and isotherms (bottom) for $B = 0.1$, $\varphi = 0.02$ and $Re = 1$

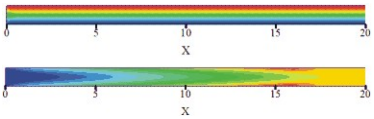

Figure 4. Streamlines (top) and isotherms (bottom) for $B = 0.1$, $\varphi = 0.02$ and $Re = 10$

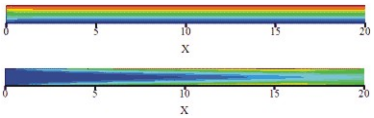

Figure 5. Streamlines (top) and isotherms (bottom) for $B = 0.1$, $\varphi = 0.02$ and $Re = 50$

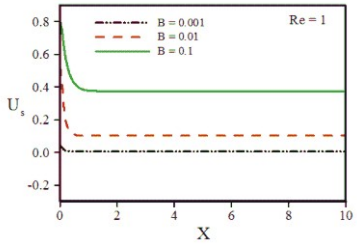

Figure 6. Slip velocity for $\varphi = 0.02$ and $Re = 1$.

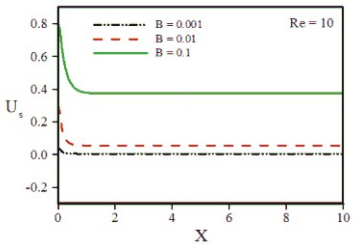

Figure 7. Slip velocity for $\varphi = 0.02$ and $Re = 10$.

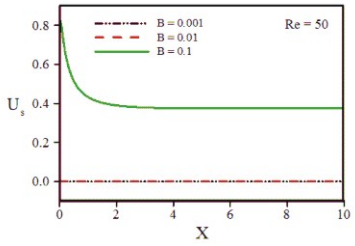

Figure 8. Slip velocity for $\varphi = 0.02$ and $Re = 50$.

The average Nusselt number $\mathrm{Nu_m}$ for different values of φ and B is presented in Figure 9, which indicates that the importance of using nanofluid to increase the heat transfer rate is distinguishable for $Re = 50$. In this case, using 4% of Cu nanoparticles leads to increase almost 11% of the average Nusselt number at $B = 0.1$. This increase is more significant (19.5%) at $B = 0.001$.

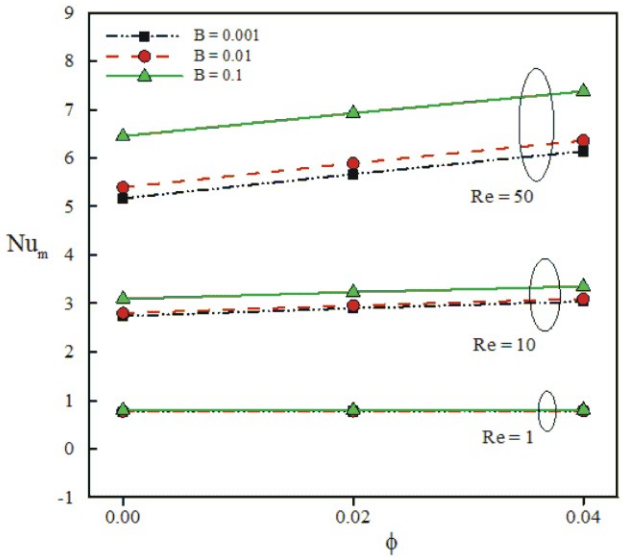

Figure 9. Average Nusselt number $\mathrm{Nu_m}$ as a function of particles concentration φ for different slip velocity coefficient and in case of Reynolds number $Re = 1$, 10 and 50

6. Conclusions

A thermal lattice Boltzmann BGK model with a dedicated boundary condition was used to study numerically laminar two-dimensional laminar forced convection heat transfer of Cu–water nanofluid

in a microchannel when he heat transfer rate is imposed at the boundaries. The effects of different volume fractions of copper nanoparticles and slip coefficient were investigated on the slip velocity and Nusselt number for $Re = 1$, 10 and 50. The results show that, as expected, heat transfer rate increases as increases the Reynolds number and the slip velocity at the wall. The effect of particle concentration is detectable for not too low values of Reynolds number and this effect is significant for the lowest slip velocity coefficient. As a result, to increase Nu in micro liquid flows, it is recommended to use nanofluid with $\varphi = 4\%$ and at low values of slip coefficient as like $B = 0.001$. The study shows that LBM together with the counter-slip thermal boundary condition can be effectively used for heat transfer phenomena in case of flows in microchannel in presence of nanofluid.

References

[1] Succi S 2001 *The lattice Boltzmann equation for fluid dynamics and beyond* (Oxford: Oxford University Press)
[2] Wang M and Kang Q 2010 Modeling electrokinetic flows in microchannels using coupled lattice Boltzmann methods *J. of Comp. Phys*. **229** 728-744
[3] D'Orazio A, Succi S and Arrighetti C 2003 Lattice Boltzmann simulation of open flows with heat transfer *Phys. of Fluids* **15** 2778-2780
[4] Nguyen N T and Wereley S T 2006 *Fundamentals and Applications of Microfluidics* (Artech House, Norwood).
[5] Bird G 1994 *Molecular gas dynamics and the direct simulation of gas flows* (Oxford).
[6] Esfe M H, Arani A A A, Karimipour A and Esforjani S S M 2014 Numerical simulation of natural convection around an obstacle placed in an enclosure filled with different types of nanofluids *Heat Transfer Res.* **45** 279–292.
[7] Aminossadati S M, Raisi A and Ghasemi B 2011 Effects of magnetic field on nanofluid forced convection in a partially heated microchannel *Int. J. Non-Linear Mech.* **46** 1373–1382.
[8] Kalteh M, Abbassi A, Saffar-Avval M and Harting J 2011 Eulerian–Eulerian twophase numerical simulation of nanofluid laminar forced convection in a microchannel *Int. J. Heat Fluid Flow* **32** 107–116.
[9] Mital M 2013 Semi-analytical investigation of electronics cooling using developing nanofluid flow in rectangular microchannels *Appl. Therm. Eng.* **52** 321–327.
[10] Raisi A, Ghasemi B, Aminossadati S M 2011 A numerical study on the forced convection of laminar nanofluid in a microchannel with both slip and no-slip conditions *Numer. Heat Transfer A* **59** 114–129.
[11] Guo Y, Qin D, Shen S and Bennacer R 2012 Nanofluid multi-phase convective heat transfer in closed domain: Simulation with lattice Boltzmann method *Int. Commun. Heat Mass Transfer* **39** 350–354.
[12] Ay C, Young C W and Young C F 2012 Application of lattice Boltzmann method to the fluid analysis in a rectangular microchannel *Comput. Math. Appl.* **64** 1065–1083.
[13] Yang Y T and Lai F H 2011 Numerical study of flow and heat transfer characteristics of alumina-water nanofluids in a microchannel using the lattice Boltzmann method *Int. Commun. Heat Mass Transfer* **38** 607–614.
[14] D'Orazio A, Karimipour A, Nezhad A H and Shirani E 2015 Lattice Boltzmann method with heat flux boundary condition applied to mixed convection in inclined lid driven cavity *Meccanica* **50** 945–962
[15] Xuan Y and Li Q 2003 Investigation on convective heat transfer and flow features of nanofluids *ASME J. Heat Transfer* **125** 151–155.
[16] Brinkman H C 1952 The viscosity of concentrated suspensions and solutions *J. Chem. Phys.* **20**

571–581.
[17] Patel H E, Sundararajan T, Pradeep T, Dasgupta A, Dasgupta N and Das S K 2005 A Micro-Convection Model for Thermal Conductivity of Nanofluids *Pramana-J. Phys.* **65** (5) 863-869.
[18] Keblinski P, Phillpot S R, Choi S U S and Eastman J A 2002 Mechanisms of heat flow in suspensions of nano-sized particles (nanofluids) *Int. J. Heat Mass Trans.* **45** (4) 855-863.
[19] D'Orazio A, Corcione M and Celata G P 2004 Application to natural convection enclosed flows of a lattice Boltzmann BGK model coupled with a general purpose thermal boundary condition *Int. J. of Thermal Sc.* **43** 575–586.
[20] D'Orazio A and Succi S 2004 Simulating two-dimensional thermal channel flows by means of a lattice Boltzmann method *Fut. Gen. Comp. Sys.* **20** 935-944.
[21] Ngoma G D and Erchiqui F 2007 Heat flux and slip effects on liquid flow in a microchannel *Int. J. Therm. Sci.* **46** 1076–1083.
[22] Karniadakis G and Beskok A 2002 *Micro flows: fundamentals and simulation* (New York).
[23] Succi S 2002 Mesoscopic modelling of slip motion at fluid-solid interfaces with heterogeneous catalysis *Phys. Rev. Lett.* **89**.